ACS APPLIED MATERIALS & INTERFACES

Research Article

www.acsami.org

Flexible Miniaturized Nickel Oxide Thermistor Arrays via Inkjet Printing Technology

Chun-Chih Huang, Zhen-Kai Kao, and Ying-Chih Liao*

Department of Chemical Engineering, National Taiwan University, Taipei 10617, Taiwan

Supporting Information

ABSTRACT: In this study, an inkjet printing process was developed to produce thermistor arrays for temperature sensing applications. First, a formulation process was carefully performed to generate a stable nanoparticle ink for nickel oxide, a material with a large temperature coefficient of resistance. The thermistor was then fabricated by printing a square NiO thin film in between two parallel silver conductive tracks on either glass plates or polyimide films. The printed thermistor, which has an adjustable dimension with a sub-millimeter scale, can operate over a wide range from room temperature to 200 °C with great sensitivity (B values ~4300 K) without hysteretic effects. When printed on polyimide films, the thermistors can also be bent or attached to curved surfaces to provide accurate and reliable temperature measurements. Moreover, the thermistor responds quickly to small temperature changes and provides an effective tool for transient temperature measurements. Finally, a thermistor array was fabricated to show the flexibility of this inkjet printing process and to demonstrate the applicability of the printed devices for temperature sensing applications.

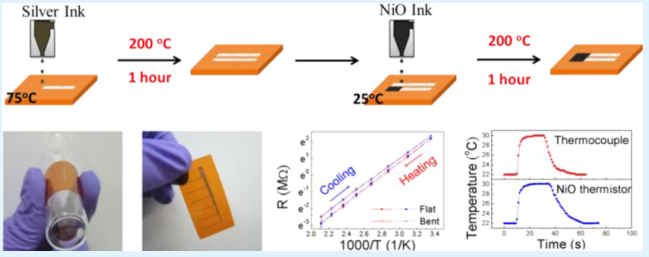

KEYWORDS: *inkjet printing technology, temperature sensing, nickel oxide, nanoparticle inks, thermistor*

INTRODUCTION

Miniaturized thermal sensors are of critical importance for dynamic temperature measurements in many mechanical or microelectronic applications, such as microchannel heat sinks,[1] IC chips,[2] and metal cutting.[3] Compared to individual temperature sensors, miniaturized temperature sensing arrays are capable of measuring the temperature distribution of a system rather than the average temperature. In order to obtain detailed thermal information on heating surfaces, a variety of temperature sensing arrays have been developed, including polysilicon thermistor arrays,[4] diode temperature sensor arrays,[5] nickel resistance temperature detector (RTD) arrays,[6] Ni−Cr thin-film thermocouple arrays,[7] and etc. However, these sensing arrays are regularly fabricated using semiconductor manufacturing technology. These processes usually require high vacuum, large power density, or a high temperature environment, which can be costly and disadvantageous for customized designs. Moreover, the creation of microscale patterns typically involves additional masking steps or an expensive lithography process and can result in the wasting of materials during the fabrication process.

On the other hand, inkjet-printing technology, a direct writing process, can form uniform and continuous thin film patterns by depositing precise amounts of inks in specific areas at room temperature and atmospheric pressure. Thus, much effort has been spent on the development of sensors, such as glucose sensors, via inkjet printing technology due to its great flexibility and precision. Recently, several inkjet-printed temperature sensors have been fabricated for temperature sensing applications. In 2011, Courbat et al.[8] inkjet-printed commercial silver nanoparticle inks on papers as Ag RTDs with dimensions of 16 mm × 16 mm. The sensor can detect temperatures between −20 and 60 °C with a temperature coefficient of resistance (TCR) of 0.11%/K. Later, Kong et al.[9] inkjet-printed square graphene thin films with dimensions of 8 mm × 8 mm on polyimide substrates for temperature sensing applications. The graphene thin films can detect a wide range of temperatures from 25 to 175 °C with a moderate sensitivity (B value of 1860 K). Although the aforementioned printed temperature sensing elements show the potential of the application of inkjet printing technology for temperature measurements, the sizes of the sensors are too large to form sensor arrays for temperature mapping on surfaces. Besides, the sensitivity needs to be improved for more precise temperature measurements.

In this study, an inkjet printing process is developed to fabricate miniaturized thermistors with high temperature sensitivity. Commercial thermistors usually need a B value above 3500 K (TCR ~ −4%/°C at 20 °C), and have sizes ranging from several millimeters to centimeters. In these commercial thermistors, nickel oxide is widely used due to its large TCR and great chemical stability.[10−14] In this study, to meet commercial standard requirements, NiO is therefore used as the temperature sensing material for printed thermistors on

Received: August 27, 2013
Accepted: December 3, 2013
Published: December 3, 2013

flexible substrates. First, NiO nanoparticle inks with great suspension stability are formulated before the lateral deposition processes. The temperature variation in the electrical resistance of the printed thermistors has been well characterized to evaluate the performance of the printed thermistors. Bending tests have also been performed to verify the flexibility and durability of the printed thermistors. Finally, printed thermistor arrays will also be fabricated and tested to show the feasibility of applying printing technology to sensor array fabrication.

EXPERIMENTAL SECTION

First, 0.5 g nickel oxide powder with primary particles of 50 nm in diameter (Sigma-Aldrich, USA) was mixed with 1 g of ethylene glycol (Sigma-Aldrich, USA) and 9 g of deionized water to form an aqueous mixture. The NiO mixture was then sonicated with a homogenizer (Sonics and Materials Inc., USA) for 10 min. Silver nanoparticles were synthesized by reducing $AgNO_3$ (Sigma-Aldrich, USA) with diethanolamine (Sigma-Aldrich, USA), as demonstrated in the literature.[15] The synthesized silver nanoparticles were centrifuged, washed, and resuspended in 30 vol % ethylene glycol aqueous solution to form a 10 wt % silver ink. Both silver and NiO inks were centrifuged again at 3000 rpm for 10 min to remove large particle aggregates before being used for inkjet printing. The ink viscosities of the silver and NiO inks at room temperature were determined by a viscometer (Brookfield DV-III) to be 7.68 and 5.92 cP, respectively. The surface tensions of the formulated inks were measured via drop shape analysis by an in-house goniometer system with a CCD camera. At room temperature, the surface tensions were 58.3 and 63.4 mN/m for silver and NiO inks, respectively.

A piezoelectric printer (JetLab 4, MicroFab, USA) was used to print patterns on glass plates or polyimide films (InTech Materials, Taiwan). Both silver and NiO inks were dispensed to form droplets of 55 μm in diameter at an ejection speed of 2.5 m/s. The printed patterns were printed with a dot spacing of 50 μm at a printing speed of 25 mm/s to form straight lines or square thin films. The deposited silver conducting lines with NiO thin films were thermally calcinated at 200 °C in a furnace for an hour.

To investigate the stability of the NiO nanoparticle ink, the NiO ink was diluted to a powder concentration of 0.1 wt %, and the pH adjustments were made by adding HNO_3 (J.T. Baker, USA) and NaOH (Mallinckrodt, USA). The dilutions with pH values ranging from 2 to 12 were then characterized by a particle size and zeta potential analyzer (Nano-ZS, Malvern). The thermal behavior of nanoparticle inks was characterized by a thermogravimetric/differential thermal analyzer (TG-DTA, TG8120, Rigaku, Japan). The microstructure of the deposit NiO thin films was examined with scanning electron microscopy (Nova NanoSEM 230, FEI, USA) with an accelerating voltage of 5 kV. The electrical resistance of the fabricated temperature sensing elements was measured in the temperature range between 50 (25) and 200 °C with a 25 °C interval using a multimeter (HP 3478A, Hewlett-Packard, USA). To examine the repeatability and reproducibility of the printed thermistors, at least five samples were tested for at least three heating/cooling cycles, and the resulting resistance data were collected to evaluate the *B* values.

RESULTS AND DISCUSSION

For printed sensors, film uniformity is crucial to product reliability, and an ink with well-suspended nanoparticles is thus needed for liquid thin film deposition. For oxide particles, surfactant or capping agents are regularly used in commercial inks to help nanoparticle suspension. However, the addition of surfactants or capping agents may lead to significant loss in temperature sensitivity for the printed NiO films, and a high temperature sintering process may be needed to remove those unwanted chemicals after the printing process. Thus, in this study, a simple pH adjustment approach is used to increase the particle suspension stability. Figure 1 showed the zeta potential

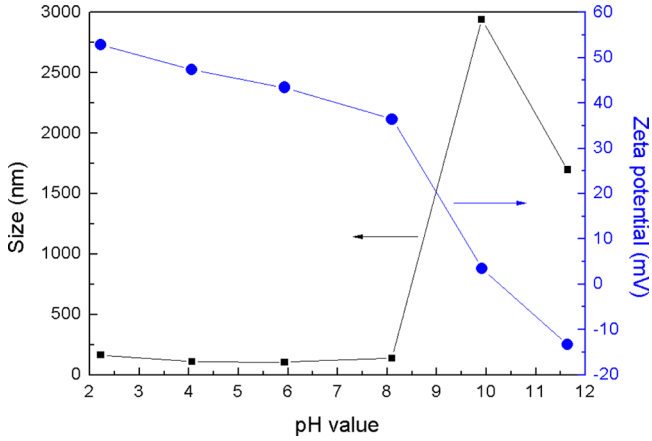

Figure 1. Variation of zeta potential (blue circles) and particle size (black squares) of NiO nanoparticle suspensions with pH values.

and particle size of NiO suspensions at various pH values. At a pH lower than 8.0, the average particle size remains nearly constant at ~200 nm. However, the zeta potential decreases slowly from 50 mV at pH 2 to 35 mV at pH 8. Although there is a gradual decrease in surface charges, the zeta potential is sufficient to provide enough electrostatic force to prevent NiO nanoparticles from aggregation. When the pH value increases to 10, the zeta potential suddenly drops to nearly zero, indicating that an isoelectric point of NiO nanoparticles is reached. Without the electrostatic barrier between particles, dramatic aggregation occurs and the average particle size increases rapidly to 3000 nm. Thus, to prepare stable NiO nanoparticle inks, extremely alkaline environments should be avoided and a pH range between 2 and 8 is favorable. However, a previous study[16] showed that the dissolution of NiO can be significant in acidic conditions (pH < 4). Therefore, a pH value of 6 was chosen in this study to prepare NiO nanoparticle inks for both chemical and suspension stability issues.

After the pH adjustment, the thermal behavior of the NiO ink was also characterized with TG-DTA to determine the ink content and the calcination temperature for printed NiO thin films. As shown in Figure 2a, more than 95% weight loss was observed before 170 °C due to the evaporation of water and ethylene glycol. Hence, a broad endothermic valley and a small

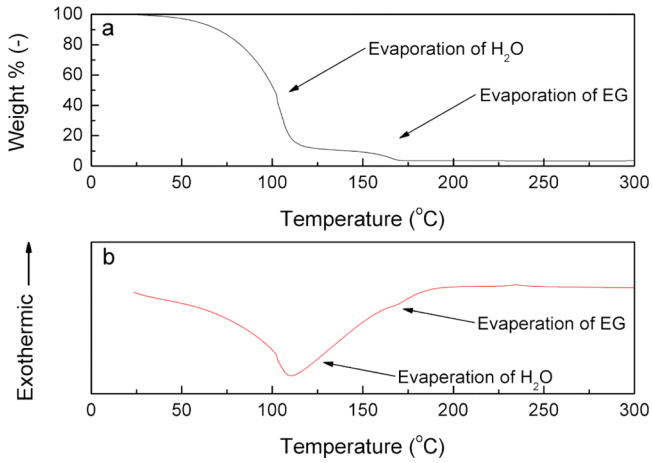

Figure 2. (a) TGA and (b) DTA curves for the NiO nanoparticle ink at an annealing ramping rate of 10 °C/min with an operating temperature up to 300 °C.

dx.doi.org/10.1021/am404872j | ACS Appl. Mater. Interfaces 2013, 5, 12954−12959

dimple at 170 °C were also observed in the DTA curve (Figure 2b) for the same temperature range. For temperatures above 170 °C, the mass remains constant at 3.5 wt %, and no peak or dimple shows up in the DTA curve, indicating that NiO nanoparticles are chemically stable below 300 °C. On the basis of these thermal analyses, a calcination temperature of 200 °C is used after NiO ink deposition to completely remove the solvents and to create compact NiO nanoparticle thin films.

The thermistor is fabricated by printing NiO and silver inks sequentially to form a complete electrical circuit for electrical resistance measurements. The effects of the printing sequence on the thermistor fabrication were first examined to ensure an effective contact between the two material stacks (NiO thin film and conductive silver tracks). In Figure 3a, a square NiO thin film was first deposited on a glass and silver tracks were then printed. To print patterns with great fidelity to the original design, the substrate was heated and kept at 70 °C.[17] Although the quick evaporation of solvent results in a NiO thin film having the same shape as the design, significant roughness, which was caused by the fast consolidation of NiO nanoparticle ink with quick evaporation, was observed. Thus, the silver tracks printed afterward became scattered and discontinuous over the NiO thin films. Moreover, the step height (~16 μm) of the NiO film leads to discontinuous silver tracks at the edges. The bad contact between NiO and silver tracks results in unreadable electrical signals after wiring the thermistor with Ag tracks on top to a multimeter. In contrast, when NiO is printed over silver tracks, a complete electrical circuit was achieved with well-defined NiO and silver thin films (Figure 3b). However, the printed NiO thin film has an uneven surface with a roughness of ~8 μm (Figure 3c) and resulted in a large electrical resistance (Table 1). The surface roughness can be substantially reduced when a lower substrate temperature (25 °C) was used. Because the evaporation rate is much slower than that at 70 °C, the gradual evaporation of solvents allows NiO nanoparticles to settle and form a compact thin film (Figure 4a). Even though the boundaries of NiO thin films expanded slightly, a smooth thin film with compact nanoparticle stacking is formed. To further investigate the microstructure, the NiO thin film was examined by scanning electron microscopy (SEM). From the SEM image (Figure 4b), NiO nanoparticles of 50 nm in diameter were closely stacked to form a compact thin film. The results of surface profilometry also show that the film had a curved surface with little roughness (Figure 4c), indicating the compact aggregation of nanoparticles in the slow evaporating process. Because the good contact between NiO

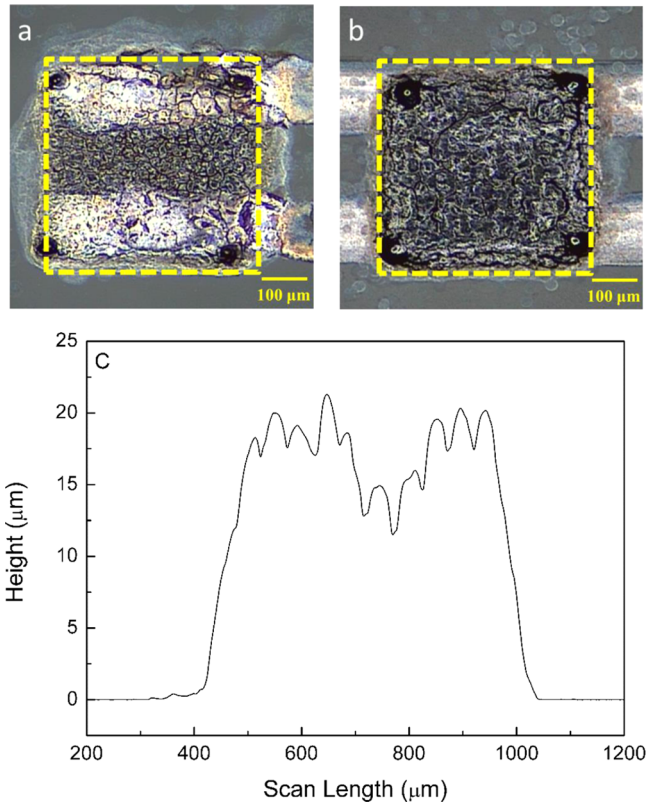

Figure 3. Comparison of printing sequence: (a) printing silver tracks over a NiO film and (b) printing NiO film over silver tracks. (c) The surface profile of the printed thermistor in part b. The glass substrate was maintained at 70 °C during the printing process. The dotted yellow lines indicate the original pattern design for the NiO thin film on a computer.

Table 1. Fabrication Parameters for the Printed Thermistors and the Corresponding *B* Values and Resistance at 50 °C

sensor	substrate temperature (°C)	thickness of NiO thin film[a] (μm)	gap between silver tracks (μm)	*B* value (K)	resistance at 50 °C (MΩ)
1	70	16.5	165	4317	48.37
2	25	13.5	165	4544	18.73
3	25	16.0	130	4337	7.06

[a]The thickness in between the two silver tracks.

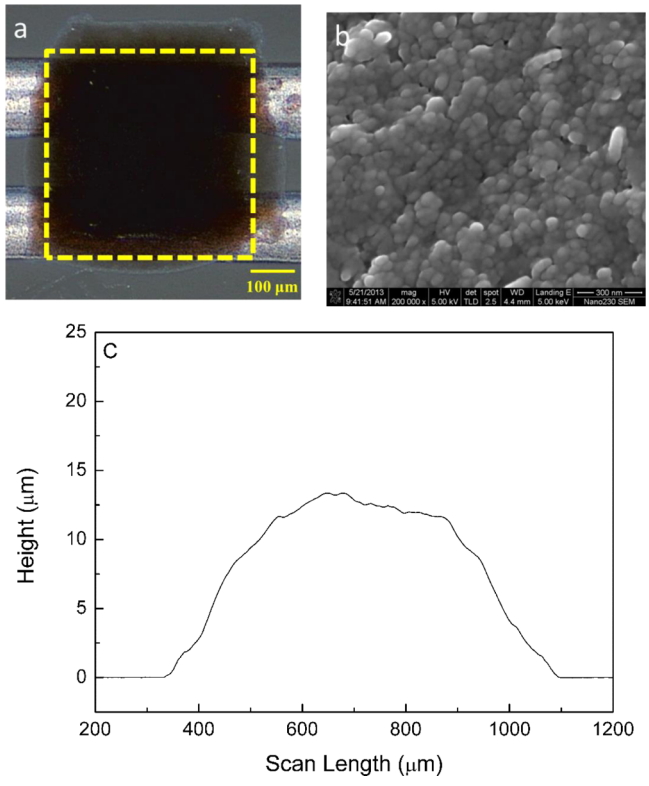

Figure 4. (a) Printed NiO film over silver tracks on a glass plate at 25 °C. Notice that the pattern is slightly larger than the original design (indicated by the dotted line). (b) The SEM image of the NiO thin film. (c) The surface profile of the printed thermistor in part a.

nanoparticles reduces the electrical conduction barrier, the resistance of this thermistor printed at 25 °C is significantly lower than the one printed at 70 °C (Table 1).

The printed thermistors possess a great temperature sensitivity and show no hysteretic effects. The printed thermistors were placed in a temperature-controlled furnace, and the transient profiles of electrical resistance with temperature variation were recorded (Figure 5). The resistance R of all the sensors decreased with the increasing temperature, and obeyed the Arrhenius relation:

$$R = R_{\infty} e^{B/T} \quad (1)$$

where R_{∞} is the resistance of the sensor at infinite temperature and B is the so-called material constant of a thermistor. The heating and cooling cycles virtually overlapped, indicating that there was almost no electrical resistance hysteresis regarding temperature variation. The resistance of the thermistor printed with a substrate temperature of 70 °C (sensor 1) was the largest among all the sensors due to the significant roughness of the NiO thin film. For the thermistor printed at 25 °C (sensor 2), as mentioned previously, the smooth and compact NiO film leads to a reduced resistance (60% smaller, see Table 1). With the design flexibility of inkjet printing technology, one can also reduce the gap distance between silver tracks or increase the thickness of NiO films to adjust the resistance of printed thermistors (sensor 3). However, because of the low substrate temperature, the areas and thicknesses of printed NiO thin films fluctuate and result in variation (Table S1, Supporting Information) of electrical resistance, which is inversely proportional to the film thickness. Regardless of the details in the fabrication process, all of the thermistors possessed great sensitivity and the B values were close to 4300 K (Table 1) with little variation (Table S1, Supporting Information), indicating that the sensitivity of the sensors depends only on the sensing material (NiO).

To test the flexibility of the printed thermistors, the electrical resistance of printed thermistors on polyimide films was measured under bending conditions (Figure 6). The polyimide films with printed thermistors were first attached to round glass bottles of different radii. The resistance of bent thermistors maintained nearly the same value as that of a flat one with a variation of less than 10%, suggesting the great flexibility and durability of the printed NiO thin films. Furthermore, the temperature variations in the electrical resistance of a thermistor under flat or bent conditions were also measured (Figure 6b or Figure S2, Supporting Information, for multiple heating/cooling cycles). The bent printed thermistor showed a slightly higher resistance than that in the flat state, possibly from the slight bending elongation of NiO thin films. However, the temperature sensitivity remained the same (both are ~4300 K), indicating that the NiO thin film remained compact with good attachment to the silver tracks. The consistent temperature sensitivity under flat or bending conditions shows not only the flexibility but also the reliability of inkjet-printed thermistors for accurate temperature measurements. Moreover, this flexibility test also implies potential applications of printed thermistors on glue tapes for temperature measurements on curvilinear surfaces.

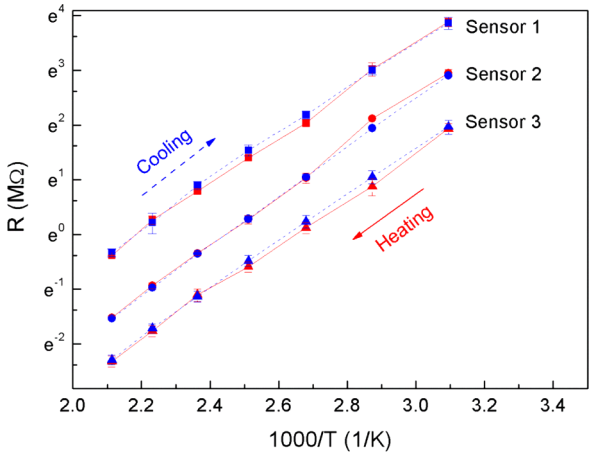

Figure 5. The variation in electrical resistance with temperature for printed thermistors on glass substrates. Three thermistors are compared here: (1) printed at a substrate temperature of 70 °C, (2) printed at a substrate temperature of 25 °C, and (3) same as (2) but with a smaller gap between silver tracks. Detailed fabrication parameters are listed in Table 1.

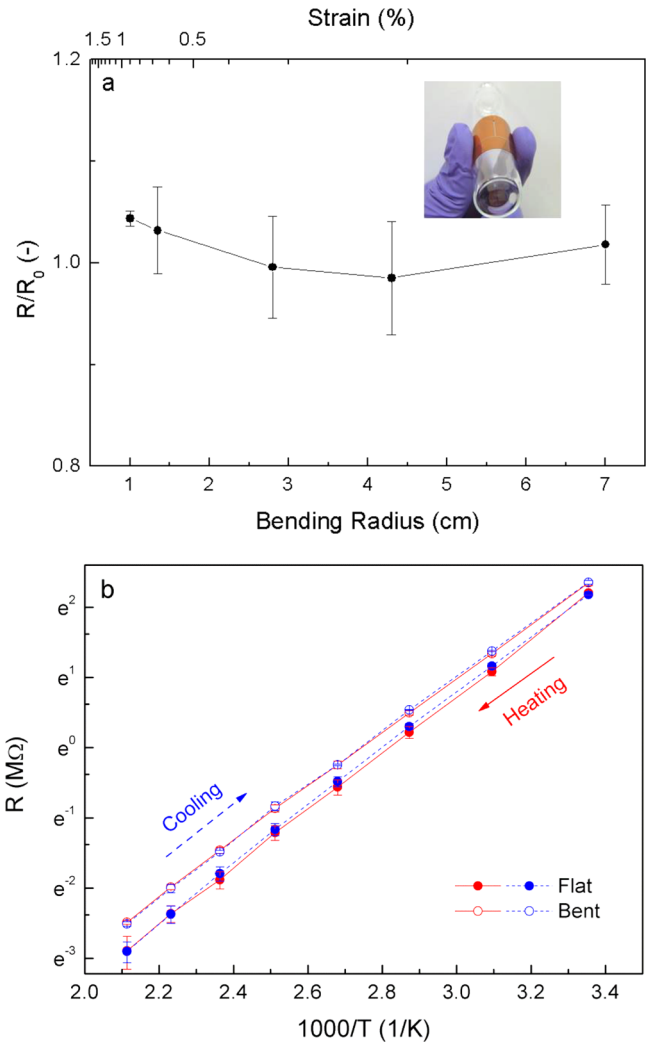

Figure 6. (a) Electrical resistance variation with the bending radius for printed thermistors on a polyimide film at 50 °C. (b) Comparison of temperature sensing performance for printed thermistors under flat and bending (bending radius = 1.35 cm) conditions. Both thermistors showed the same sensitivity without any hysteresis, but the bent thermistor has a slightly higher resistance.

dx.doi.org/10.1021/am404872j | ACS Appl. Mater. Interfaces 2013, 5, 12954−12959

The printed thermistor has a fairly fast response time and is able to measure temperature changes with great precision. The responses of printed thermistors to temperature changes were evaluated by a finger touch experiment. The sensors were first held by gloved human fingers until the equilibrium state of ~30 °C was reached, and were then released to the ambient environment (22 °C). The electrical resistance variation that resulted from the touch of a fingertip was translated to temperature variation and was shown in Figure 7. In comparison, the response of a K-type thermocouple probe of ~1 mm diameter was also recorded. Upon finger touch, either the printed thermistors or thermocouple reacted quickly to the temperature change in less than 1 s. Then, heat was gradually transferred from the finger to the temperature sensing devices, and an equilibrium temperature was reached at 30 °C. The printed thermistor on polyimide showed a similar equilibrium time scale as that of the thermocouple, but the thermistor on glass took a longer time to reach the equilibrium state than the other two sensors, possibly because of the larger heat capacitance of the glass substrate. Moreover, the larger heat capacitance of the glass substrate also leads to a long recovery time after removing the finger touch (6 min). On the other hand, when inkjet-printed on a thin polyimide film, the NiO thermistor reacted almost as fast as the thermocouple did. The equilibrium and recovery times were both significantly reduced due to a substantial decrease in the substrate heat capacitance, which was helpful for the heat transfer. Therefore, to measure the temperature distribution on surfaces with attached printed thermistors, one should carefully select a thin substrate with a low heat capacity in order to obtain quick responses and accurate measurements.

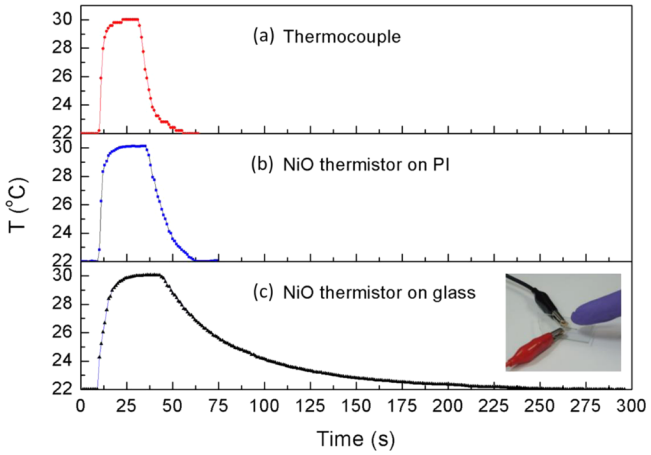

Figure 7. Responses of different temperature sensors during the touch and leave process of the fingertip: (a) K-type thermocouple, (b) printed thermistor on PI, and (c) printed thermistor on glass. The inset picture shows the experimental setup.

With the flexibility of inkjet printing technology, the thermistors can be allocated in different positions easily with various circuit layouts. Figure 8 shows two designs of 3 × 1 thermistor arrays on various substrates. The dimensions of each sensing element are about 0.5 mm × 0.5 mm, which is as small as commercial miniature thermistors. In order to test the performance of the inkjet-printed thermistor arrays, a solder iron with a surface temperature of 230 °C was applied 2 mm away from a row of three thermistors, which were equally spaced 2 mm apart on a glass plate (see the inset picture in Figure 9). As shown in Figure 9, the temperature at the

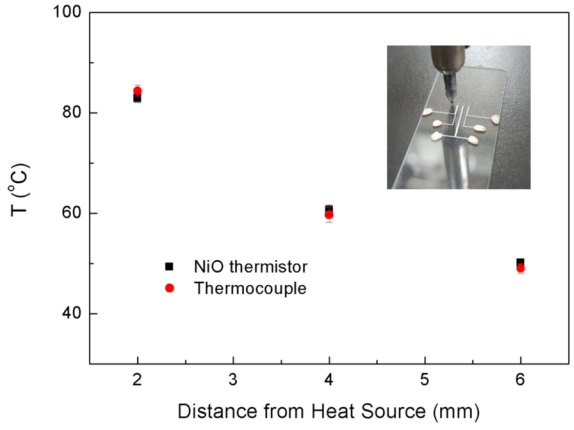

Figure 9. Temperature distribution around a solder iron detected by the inkjet-printed thermistor array and thermocouples. The inset picture shows the experimental setup.

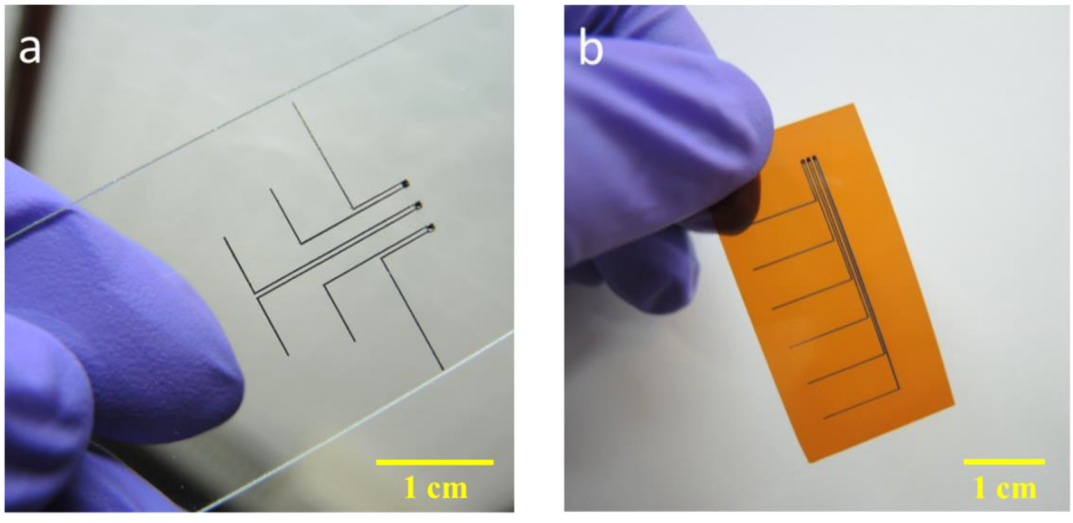

Figure 8. Optical images of printed thermistor arrays on (a) glass substrates and (b) polyimide substrates.

position 2 mm from the heat source was 83.2 °C and decreased to 60.6 and 50.2 °C as the distance increased to 4 and 6 mm, respectively. The measured temperature distribution was in good agreement with the results obtained from a thermocouple at the same positions, suggesting the feasibility and accuracy of the inkjet-printed thermistor array on temperature distribution measurements.

CONCLUSIONS

An inkjet printing process was developed for miniaturized NiO thermistor arrays on flexible substrates for temperature sensing applications. Nickel oxide nanoparticles were well suspended in 10 wt % ethylene glycol aqueous solution at pH 6 to form a stable particle ink. On the basis of the thermogravimetric results, a calcination temperature of around 170 °C is needed to completely remove the ink solvents for NiO nanoparticle deposition. Therefore, after NiO inks were printed on substrates, the deposited patterns were heated at 200 °C for an hour before use. To avoid fracture or disconnections of silver tracks around the edges of NiO thin films, silver tracks were printed before/below the NiO thin films to form complete electrical circuits. During the printing process, when a high substrate temperature (70 °C) is used, the printed NiO films have good shape definitions but possess significant surface roughness. In contrast, with a low substrate temperature (25 °C), the printed NiO film forms a uniform layer of nanoparticle packing and possesses lower electrical resistance. By shortening the distance between the silver tracks and increasing the thickness of the NiO films, one can also reduce or adjust the resistance of the printed thermistors. Despite the different printing procedures, all of the printed thermistors possess very high temperature sensitivity (B values ~4300 K) without thermal hysteresis. When printed on flexible polyimide substrates, the thermistors preserved the same temperature sensing performance under bending conditions showing good reliability of the printed thermistors. The response time of the printed thermistors was almost as fast as that of the thermocouples. However, the equilibrium time was found to be related to the thermal capacity of the substrate and can be significantly reduced with thinner substrates. An inkjet-printed thermistor array was also fabricated to demonstrate the ability of printed sensors for temperature distribution measurements with great precision. In summary, this study shows the applicability of printing- or solution-based processes for miniaturized flexible sensing devices instead of traditional coating/etching processes. With the flexibility of inkjet printing technology, the sensor location and circuit layouts can be adjusted easily to form a sensor array for temperature distribution measurements. This fast fabrication route for flexible thermistor arrays shows the capability of printed devices and opens a new avenue for potential sensing applications in printed electronics.

ASSOCIATED CONTENT

Supporting Information

This section includes particle size analysis for the silver ink, performance of the printed thermistor under multiple temperature variation cycles, optical and SEM images of the printed thermistor after bending, and the statistics of characteristic parameters for the printed thermistors. This material is available free of charge via the Internet at http://pubs.acs.org.

AUTHOR INFORMATION

Corresponding Author

*Phone: 886-2-3366-9688. Fax: 886-2-2362-3040. E-mail: liaoy@ntu.edu.tw.

Notes

The authors declare no competing financial interest.

ACKNOWLEDGMENTS

This research was supported by the National Science Council in Taiwan through Grants NSC 101-2221-E-002-177-MY2 and NSC 102-2218-E-002-006.

REFERENCES

(1) Jang, S. P.; Kim, S. J.; Paik, K. W. *Sens. Actuators, A* **2003**, *105*, 211−224.
(2) Liu, H. X.; Sun, W. Q.; Xiang, A.; Shi, T. W.; Chen, Q.; Xu, S. Y. *Nanoscale Res. Lett.* **2012**, *7*, 1−6.
(3) Li, K.-M.; Liang, S. Y. *J. Manuf. Sci. Eng.* **2005**, *128*, 416−424.
(4) Xue, Z. L.; Qiu, H. H. *Sens. Actuators, A* **2005**, *122*, 189−195.
(5) Han, I. Y.; Kim, S. J. *Sens. Actuators, A* **2008**, *141*, 52−58.
(6) Binghe, M.; Jinzhong, R.; Jinjun, D.; Weizheng, Y. *Flexible thermal sensor array on PI film substrate for underwater applications.* IEEE 23rd International Conference on Micro Electro Mechanical Systems (MEMS), Hong Kong, 2010.
(7) Liu, H. X.; Sun, W. Q.; Chen, Q.; Xu, S. Y. *IEEE Electron Device Lett.* **2011**, *32*, 1606−1608.
(8) Courbat, J.; Kim, Y. B.; Briand, D.; de Rooij, N. F. *Inkjet printing on paper for the realization of humidity and temperature sensors*. 16th International Conference on Solid-State Sensors, Actuators and Microsystems, Beijing, China, 2011.
(9) Kong, D.; Le, L. T.; Li, Y.; Zunino, J. L.; Lee, W. *Langmuir* **2012**, *28*, 13467−13472.
(10) Aleksic, O. S.; Nikolic, M. V.; Lukovic, M. D.; Nikolic, N.; Radojcic, B. M.; Radovanovic, M.; Djuric, Z.; Mitric, M.; Nikolic, P. M. *Mater. Sci. Eng., B* **2013**, *178*, 202−210.
(11) Kang, J. E.; Ryu, J.; Han, G.; Choi, J. J.; Yoon, W. H.; Hahn, B. D.; Kim, J. W.; Ahn, C. W.; Choi, J. H.; Park, D. S. *J. Alloys Compd.* **2012**, *534*, 70−73.
(12) Ko, S. W.; Schulze, H. M.; Saint John, D. B.; Podraza, N. J.; Dickey, E. C.; Trolier-McKinstry, S. S. *J. Am. Ceram. Soc.* **2012**, *95*, 2562−2567.
(13) Ryu, J.; Kim, K. Y.; Choi, J. J.; Hahn, B. D.; Yoon, W. H.; Lee, B. K.; Park, D. S.; Park, C. *J. Am. Ceram. Soc.* **2009**, *92*, 3084−3087.
(14) Schulze, H.; Li, J.; Dickey, E. C.; Trolier-McKinstry, S. *J. Am. Ceram. Soc.* **2009**, *92*, 738−744.
(15) Ahn, B. Y.; Duoss, E. B.; Motala, M. J.; Guo, X. Y.; Park, S. I.; Xiong, Y. J.; Yoon, J.; Nuzzo, R. G.; Rogers, J. A.; Lewis, J. A. *Science* **2009**, *323*, 1590−1593.
(16) Hernandez, N.; Moreno, R.; Sanchez-Herencia, A. J.; Fierro, J. L. G. *J. Phys. Chem. B* **2005**, *109*, 4470−4474.
(17) Jeong, S.; Song, H. C.; Lee, W. W.; Choi, Y.; Ryu, B. H. *J. Appl. Phys.* **2010**, *108*, 102805.